Intravascular Water Molecule Lifetime in the Japanese Macaque Brain

J. M. Njus[1], J. R. Pollaro[1], M. T. Snodgrass[1], J. Cunneen[1], E. Muldoon[1], V. B. Warren[2], X. Li[1], C. S. Springer[1], S. G. Kohama[2], and W. D. Rooney[1]

[1]Advanced Imaging Research Center, Oregon Health & Science University, Portland, OR, United States, [2]Oregon National Primate Research Center, Beaverton, OR, United States

Introduction: Non-human primate (NHP) models of cerebral pathology are important for development and efficacy of new treatment therapies.[1-3] Interestingly, the remarkable physiological connection between NHPs and humans has not been investigated using dynamic contrast-enhanced (DCE) MRI. DCE-MRI measurements using gadolinium (Gd) based contrast reagents (CRs) are useful for characterizing the blood vessel properties in human brain tissue,[4-11] and are sensitive to disease-related changes in vascular properties.[10,11] Physiologically important parameters, such as blood-brain barrier (BBB) permeability, blood volume, and transendothelial water exchange have been examined in normal human brain,[5-8] but not in NHP. In this study, we use DCE MRI to investigate BBB permeability (K^{trans}), blood volume fraction (v_b), and the intravascular water lifetime (τ_b) in Japanese macaque brain.

Methods: All animal care and experimental procedures were IACUC-approved. Ten Japanese macaques (JMs) (4 males, 6 females, ages 7.7-19.6 yr) were selected from a free-ranging colony maintained by our institution. All MR data were collected with a 3T MRI Instrument (Siemens TRIO) using a quadrature transmit/receive extremity RF coil. Animals were initially sedated with Telazol, intubated and maintained on 1% isoflurane in 100% O_2 during the MRI study. The animals were continuously monitored by pulse oximetry, respiration, and end tidal $C0_2$. Five full volume parametric ^1H_2O T_1 maps were produced at different times relative to CR administration by voxel-wise fittings of four consecutively acquired IR-MPRAGE turboFLASH acquisitions (3D TFL: TR/TE = 2500/3.49 msec; FA = 8°) collected with different inversion times (TI = 200, 900, 2000 ms, and also with no inversion pulse). ^1H_2O T_1 maps were produced by numerically evaluating the Bloch equations for the variable TI data set accounting for all RF pulses and delays with the constraint that each voxel exhibited a monoexponential IR recovery. For DCE measurements, a 0.2 mmol/kg dose of Gd (Gadoteridol, Bracco Diagnostics, Inc) was administered at 0.5 mL/sec using an infusion pump. For each animal, a pre-Gd T_1 map, and four post-Gd T_1 maps were collected at ~6.8, ~17.5, ~28.3, and ~42.7 min. (time values represent the approximate time from CR injection to the acquisition mid-points). The T_1 maps were then masked (performed manually for each animal) to select the entire brain. White matter (WM) and gray matter (GM) T_1 values were obtained from fitting the two prominent peaks in the full volume T_1 histograms to a Gaussian function. BBB Gd permeability was determined as K^{trans} (the volume transfer rate constant for CR across the BBB)[4,5], blood volume fraction as v_b (%), and transendothelial exchange was characterized by the mean residence lifetime of the blood water molecule, τ_b (ms). K^{trans}, v_b, and τ_b were determined from multi-parameter fittings of the pre- and post-Gd WM histogram R_{1t} [$\equiv 1/T_1$] peak values to a two compartment model [for blood plasma and the extracellular-extravascular space (EES)] that also accounts for equilibrium transendothelial exchange of molecular water.[8-11]

Results and Discussion: Administration of Gd decreases T_1 in JM WM (**Figure 1**). The temporal WM T_1 change results from the Gd concentration changes in the plasma and EES (due to nonzero K^{trans}) spaces, and also from trans-BBB water exchange. The influence of CR leakage (K^{trans}) is shown in **Figure 2**, where for nonzero K^{trans}, the R_{1t} is elevated at any point in time. Though small, a nonzero K^{trans} can result in substantial v_b and τ_b errors if they are calculated assuming $K^{trans} = 0$. In one JM, fitting[8,9] R_{1t} *vs.* R_{1b} yielded v_b and τ_b values of ~2.8% and ~430 ms, respectively, for zero K^{trans}, and ~2.5% and ~299 ms for $K^{trans} = 5.5 \times 10^{-5}$ min^{-1} (**Figure 3**). **Table 1** lists the uncorrected and corrected (*via* the group mean K^{trans}) v_b and τ_b values for each macaque. The mean WM K^{trans} (~5.5×10^{-5} min^{-1}) and corrected τ_b (~300 ms) values in the sedated JM are very similar to K^{trans} (~2×10^{-5} min^{-1})[11] and τ_b (~260 ms)[9] in conscious humans, whereas the mean JM v_b (~2.5%) value is somewhat greater than human v_b (~1.4%)[9,11]. Fitting precision improved after correcting the data for CR extravasation.

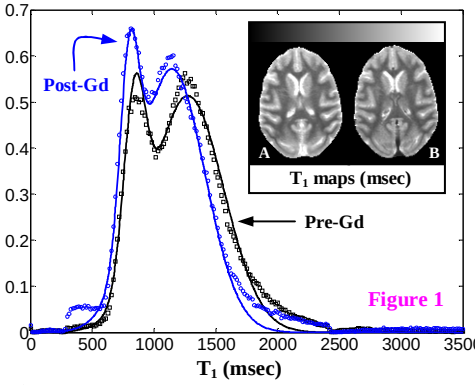

Table 1. Pharmacokinetic parameters: v_b, and τ_b

N	Sex	v_b (%)	v_b (%)†	τ_b (msec)	τ_b (msec)†
1	F	3.2	2.9	294	296
2	F	2.8	2.5	428	299
3	F	3.0	2.8	528	296
4	F	2.3	2.1	308	304
5	F	1.9	1.6	310	128
6	F	4.3	4.0	282	152
7	M	3.2	3.1	289	291
8	M	3.4	3.0	291	293
9	M	1.3	1.4	973	654
10	M	2.0	2.0	898	310
Avg. (± SE):		2.7 (± 0.3)	2.5 (± 0.3)	469 (± 76)	302 (± 44)

† Corrected using $K^{trans} = 5.5 \times 10^{-5}$ min^{-1}

Figure 1. Full volume T_1 histogram values and fittings produced from the pre-Gd and (~6.8 min) post-Gd T_1 data sets of a 19.2 yr old female macaque. The inset (upper right corner) displays two T_1 maps, the map on the left (A) is a slice from the pre-Gd data, and the map on the right (B) is the same slice from the post-Gd data. The T_1 values in the maps are represented by the grayscale (0-2000 ms) located above the maps.

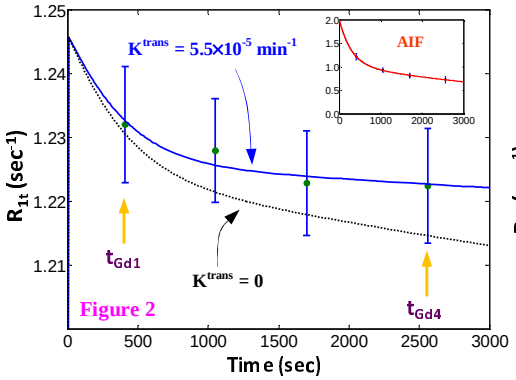

Figure 2. WM R_{1t} [$\equiv 1/T_1$] vs. time. The R_{1t} data in the graph represent the group mean R_{1t} values (±SE) across the pharmacokinetic time series. Displayed are the curves obtained from fitting the R_{1t} data to a model that allows for subtle CR leakage across the BBB ($K^{trans} > 0$), and without CR leakage ($K^{trans} = 0$). The difference between the two curves increases with time: The inset (upper right corner) displays the arterial input function [AIF; $C_p(t)$ (mM)].

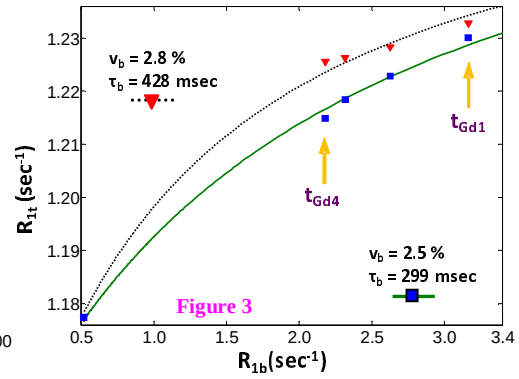

Figure 3. WM R_{1t} vs. R_{1b} data and fittings obtained from a 16.7 yr old female JM subject. Displayed are the curves obtained from R_{1t} vs. R_{1b} fittings of the (uncorrected; $K^{trans} = 0$) R_{1t} data (▼), and the R_{1t} data (■) corrected for CR leakage ($K^{trans} > 0$). Parameters (v_b and τ_b) produced from the fittings are shown in the corners of the figure. The difference between the uncorrected and K^{trans}-corrected R_{1t} values with time is proportional to the difference in the $R_{1t}(t)$ curves in Figure 2 (see labels t_{Gd1},t_{Gd4})

References: **1.** Hart, et. al., *Drug Discov. Today* 11;58-66 (2006). **2.** Blezer, et. al., *NMR Biomed.* 181;545-547 (1991). **3.** LaVerde, et. al., Magn. Reson. Med. 57;201-205 (2007). **4**. Tofts, et. al., *Magn. Reson. Med.* 17;357-367 (1991). **5**. Tofts, *J. Magn. Reson. Imaging* 7;91-101 (1997). **6**. Donahue, et. al., *Magn. Reson. Med.* 36;858-867 (1996). **7**. Schwarzbauer, et. al., *Magn. Reson. Med.* 37;769-777 (1997). **8**. Rooney, et. al., *PISMRM* 11;2188 (2003). **9**. Rooney, et. al., *PISMRM* 11;1390 (2004). **10**. Njus, et. al., *PISMRM* 15;2193 (2007). **11**. Njus, et. al., *PISMRM* 16;3431 (2008).

Grant Support: OHSU/Vertex, SRA-05-07-1, NIH RO1-EB007258, NIH: RO1-NS40801, RO1-EB00422